


ARTICLE

Bioactivity improvement via display of the hydrophobic core of HYD1 in a cyclic β -hairpin-like scaffold, MTI-101

Priyesh Jain^{1,2,3} | David B. Badger^{1,2} | Yi Liang¹ | Anthony W. Gebhard⁴ | Daniel Santiago¹ | Philip Murray¹ | Sridhar R. Kaulagari^{4,5} | Ted J. Gauthier¹ | Rajesh Nair⁴ | MohanRaja Kumar¹ | Wayne C. Guida^{1,2} | Lori A. Hazlehurst^{3,4,5} | Mark L. McLaughlin^{1,4,5,6} 

¹Department of Chemistry, University of South Florida, Tampa, Florida, USA

²Drug Discovery Department, H. Lee Moffitt Cancer Center & Research Institute, Tampa, Florida, USA

³Modulation Therapeutics Incorporated, Morgantown, West Virginia, USA

⁴Tumor Biology Department, H. Lee Moffitt Cancer Center & Research Institute, Tampa, Florida, USA

⁵Department of Pharmaceutical Sciences, West Virginia University Health Sciences Center, Morgantown, West Virginia, USA

⁶Department of Chemistry, West Virginia University, Morgantown, West Virginia, USA

Correspondence

Mark L. McLaughlin, Department of Pharmaceutical Sciences, West Virginia University, 64 Medical Center Drive, Morgantown, WV 26506-9530, USA. Email: mark.mclaughlin@hsc.wvu.edu

Present address

Ted J. Gauthier, AgCenter Biotechnology Laboratory, LSU Agricultural Center, Baton Rouge, Louisiana, USA

Funding information

Multiple Myeloma Research Foundation; National Cancer Institute, Grant/Award Numbers: 5R01CA195727, 5R44CA22155

Abstract

HYD1 is an all D-amino acid linear 10-mer peptide that was discovered by one-bead-one-compound screening. HYD1 has five hydrophobic amino acids flanked by polar amino acids. Alanine scanning studies showed that alternating hydrophobic amino acid residues and N- and C-terminal lysine side chains were contributors to the biological activity of the linear 10-mer analogs. This observation led us to hypothesize that display of the hydrophobic pentapeptide sequence of HYD1 in a cyclic beta-hairpin-like scaffold could lead to better bioavailability and biological activity. An amphipathic pentapeptide sequence was used to form an antiparallel strand and those strands were linked via dipeptide-like sequences selected to promote β -turns. Early cyclic analogs were more active but otherwise mimicked the biological activity of the linear HYD1 peptide. The cyclic peptidomimetics were synthesized using standard Fmoc solid phase synthesis to form linear peptides, followed by solution phase or on-resin cyclization. SAR studies were carried out with an aim to increase the potency of these drug candidates for the killing of multiple myeloma cells *in vitro*. The solution structures of **1**, **5**, and **10** were elucidated using NMR spectroscopy. ¹H NMR and 2D TOCSY studies of these peptides revealed a downfield H _{α} proton chemical shift and 2D NOE spectral analysis consistent with a β -hairpin-like structure.

1 | INTRODUCTION

Multiple myeloma (MM) develops solid tumors in the bone marrow microenvironment due to interactions with cell adhesion receptors involved in cell-cell and cell-extracellular matrix interactions. MM tumors thrive in the bone marrow microenvironment due to access

to growth factors that are secreted from neighboring stromal cells that normally nurture developing hematopoietic cells.^[1-4] Bone marrow metastasis is common for many solid tumors such as prostate, lung, and breast. MM and metastatic prostate cancer progression involves bone marrow disease in 100% and 92% of patients, respectively.^[5-9] Herein, we describe the synthesis of cyclized

This is an open access article under the terms of the Creative Commons Attribution-NonCommercial-NoDerivs License, which permits use and distribution in any medium, provided the original work is properly cited, the use is non-commercial and no modifications or adaptations are made.

© 2020 The Authors. *Peptide Science* published by Wiley Periodicals LLC.

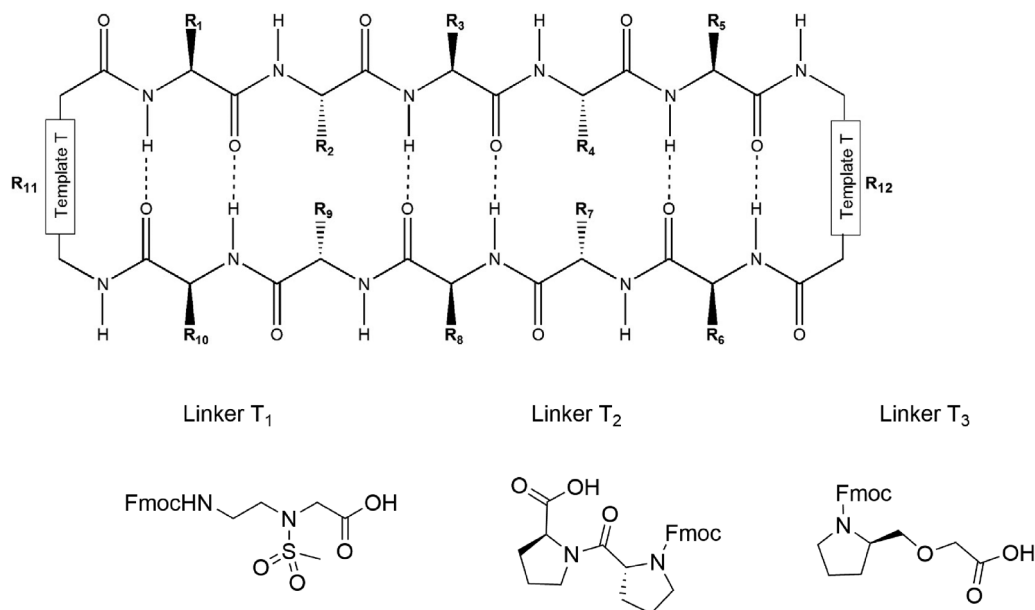


FIGURE 1 Cyclic HYD1 proteomimetic scaffold with novel T₁, T₂, and T₃ turn promoters (linkers)

peptidomimetic (Figure 1) of the previously reported linear all *D*-amino acid peptide, HYD1.^[10–14] We have developed a molecule with commercial potential to treat MM and have named our lead compound, **10**, MTI-101. MTI-101 kills MM cell lines and has promising *in vivo* activity in two different murine models of MM.^[8] The mechanism of cell killing by MTI-101 is not fully elucidated, but calcium overload or captopsis is consistent with the available data.^[15,16]

2 | MATERIALS AND METHODS

Organic and inorganic reagents (ACS grade) were obtained from commercial sources and used without further purification, unless otherwise noted. Fmoc-protected amino acids and the coupling agent HCTU were obtained from Protein Technologies, Calbiochem-Novabiochem, or Chem-impex International. 2-Chlorotrityl chloride resin was purchased from Anaspec Inc. All linear peptides were synthesized on the Symphony peptide synthesizer, Protein Technologies Instruments. Solvents for peptide synthesis and reverse-phase HPLC were obtained from Applied Biosystems. Other chemicals used were obtained from Aldrich and were of the highest purity commercially available. Thin layer chromatography (TLC) was performed on glass plates (Whatman) coated with 0.25 mm thickness of silica gel 60 Å (#70–230 mesh). High-resolution mass spectra were obtained on an Agilent LC-MSD-TOF.

2.1 | Circular dichroism measurement

Circular dichroism (CD) experiments were carried out at room temperature on the Aviv (Model # 210) spectropolarimeter flushed with nitrogen. The samples were prepared as stock solutions in sodium acetate buffer

and diluted to the desired concentration for measurements. Each spectrum was collected from 250 to 184 nm using a 0.1 cm path length cylindrical quartz cell. Each spectrum was recorded as an average of three scans taken at a spectral bandwidth of 1 nm. All spectra were corrected for buffer contributions and presented in units of molar ellipticity.

2.2 | NMR spectroscopy

All deuterated reagents and solvents were purchased from Cambridge Isotopes. All 1D ¹H and ¹³C NMR spectra were recorded on a Bruker 250 MHz or a Varian INOVA 400 MHz spectrometer in CDCl₃ unless otherwise specified and chemical shifts are reported in ppm (δ) relative to internal standard tetramethylsilane (TMS). 2D NMR samples were prepared by dissolving 1 to 2 mg peptide in 100 μ L D₂O and then adjusting the pD to 4.0 (uncorrected) with either 50 mM NaOAc-*d*₃ or 50 mM AcOH-*d*₄ to yield a final concentration between 3 and 7 mM. Chemical shifts are reported in parts per million (ppm) relative to 0.5 mM DSS. NMR experiments were run and processed on a three-channel Varian Inova 500 MHz instrument at 298.1 K using a 3-mm I.D. RT probe equipped with Z-axis PFGs running VnmrJ 2.2D. Spectra were then analyzed using ACD labs NMR Manager version 11.0. 1D NMR spectra were collected using 32 K data points, between 16 and 64 scans were collected using a 0.5 second delay and 1 second presaturation. 2D TOCSY and NOESY experiments were run with a 5000 Hz window in both dimensions. TOCSY experiments were run with a mixing time of 60 ms, a 0.5 second relaxation delay followed by 1 second of presaturation and 512 increments in the *f*₁ dimension with 32 transients per increment (collecting 4096 data points per transient in the *f*₂ dimension). Zero-filling was then applied using 4096 points for each dimension. NOESY experiments were performed using a 500 ms mixing time, 1 second of presaturation and

512 increments of 32 transients each (collecting 4096 data points per transient in the f_2). Zero-filling was then applied using 4096 points for each dimension. Presaturation was used to suppress the water resonance both during the relaxation delay and during the mixing time. All spectra were analyzed using standard window functions (Gaussian without shifting).

2.3 | Constrained conformation search with MacroModel

Structures were created with Maestro 8.5 for peptides **1** and **5**. Minimizations of the structures were performed with MacroModel 9.8.^[17,18] The OPLS 2005 force field was used with implicit water and a constant dielectric constant of 1.0 while using the Truncated Newtonian Conjugate Gradient algorithm with a threshold of 0.01 kJ/mol.^[19] A Mixed Monte Carlo Multiple Minimum (MCM)/Low-Mode Conformational Search (LMCS) method was employed with NOEs data, which were introduced as flat-bottom energetic restraint wells to yield a constrained potential energy. Torsion angles were similarly restrained for all peptide bonds. A 200 kJ/mol energy window of structures were kept during the conformation search where only structures in the lower 100 kJ/mol were outputted. Redundant conformations were eliminated and 20 lowest energy structures were kept for analysis.

2.4 | Cell viability assay

NCI-H929 MM cell line was purchased from ATTC (Rockfield, MD). Cell lines were authenticated by Mycoplasma testing every 6 months and STR analysis once a year. Cells were maintained at 37 °C in 5% CO₂ in RPMI media containing 10% FBS. Cells grown in log phase were plated at a density of 400,000 cells/ml and were treated with varying concentrations of the indicated peptide or vehicle control for 24 hours. Following peptide treatment, cells were centrifuged at 1200 rpm for 5 minutes at 4 °C and washed twice in cold PBS. Cells were stained with 2 nM TOPRO3 iodide and analyzed with the BD FACS Calibur and FlowJo software. The assay was done in triplicate and repeated three times. The IC₅₀ values were calculated using linear regression analysis.

3 | RESULTS AND DISCUSSION

3.1 | Peptide design

Using combinatorial peptide libraries and a functional binding assay, Cress, Lam, and colleagues identified several peptides that inhibited $\alpha 2\beta 1$ and $\alpha 6\beta 1$ integrin mediated adhesion of prostate cancer cells to fibronectin, laminin, and collagen IV.^[10] They specifically identified an all *D*-amino acid containing peptide referred to as HYD1 (kikmviswkg) that blocks binding of epithelial prostate carcinoma cells to extracellular matrix components.^[11] Hazlehurst and co-workers truncated the N- and C-termini and alanine scan studies identified the highlighted

side chains **mvisw** as the critical side chains for the *in vitro* cell killing activity of HYD1 according to the TOPRO3 assay described below (see Table S10).^[15] The alternation of side chain residues important to the *in vitro* cell killing activity suggested that the active conformation for this activity was an extended conformation since that conformation would display those three side chains along a single strand and in the same direction. Using this information and the finding that Val for Ile replacement gave a slightly more active HYD1 analog, we synthesized a cyclized version of HYD1 that was designed to display the core sequence (MVVSW) in one strand and (KLKLLK) as an amphipathic anti-parallel strand. We also reasoned that the pentapeptide sequence (KLKLLK) would maintain good solubility. It was also thought that the amphipathic display of the polar side chains in that strand would stabilize the anti-parallel β -sheet-like conformation for the resulting peptidomimetic. The N- to C- terminal cyclization of the linear peptides was done to restrict the number of conformations available to the linear peptide, which increases the affinity of the cyclized peptide for its target when the constraint stabilizes the bound conformation of the peptidomimetic. We synthesized the cyclic *D*-HYD1 analog using a novel methyl sulfonamide aminoethyl glycine linker **T₁** that connects the two anti-parallel strands. The first cyclic HYD1 analog retained all of the *D*-amino acids and used a *L*-Pro-*D*-Pro β -turn promoter, which is the enantiomeric form of the well-known *D*-Pro-*L*-Pro beta-turn promoter for β -hairpin peptides.^[20,21] This cyclic β -hairpin analog was found to be twice as active as linear HYD1 against H929 cells. The *inverso* cyclic HYD1 peptide analog (peptide **2**, Table 1) having all *L* amino acids except for the enantiomeric *D*-Pro-*L*-Pro beta-turn promoter was subsequently investigated for its potential to kill MM cell lines. Peptide **2** was twice active as HYD1 analog.

3.2 | Structure-activity relationship (SAR) studies for cyclic HYD1 peptides

In an effort to optimize the bioactivity of cyclic HYD1, it was essential to determine the key residues most critical to the bioactivity of the cyclic HYD1 peptides. As shown in Table 1, bioactivity data of cyclic HYD1 peptide analogs (peptides **3-7**) revealed Trp, Val₂, and Met in peptides **3**, **5**, and **7**, respectively as residues critical to the bioactivity. Replacement of the Ser residue with the more hydrophobic Ala in peptide **4** significantly improved the bioactivity of the cyclic HYD1 analog and more hydrophobic amino acids replacing that alanine maintained or decreased bioactivity. Oxidation of Met side chain was observed during peptide isolation for some cyclic HYD1 analogs. This problem was overcome by replacing the Met side chain with, a structurally similar and chemically stable side chain, Nle. Fortunately, introduction of the Nle into the hydrophobic strand of peptide **8** resulted in a further increase of the peptide's bioactivity. Next efforts were made to further enhance the bioactivity by making slight changes such as increasing the hydrophobicity or slightly decreasing the hydrophobicity of the WAVVN* strand. Cress and co-workers have previously reported that another peptide RZ-3 (kmviywkg) similar to HYD1 inhibited adhesion of prostate tumor cells to extracellular matrix

TABLE 1 Structure-activity relationship studies of HYD1 and cyclic HYD1 peptide analogs

Peptide	R ₁	R ₂	R ₃	R ₄	R ₅	R ₆	R ₇	R ₈	R ₉	R ₁₀	R ₁₁	R ₁₂	IC ₅₀ (μ M)	SD
HYD1	K	I	K	M	V	I	S	W	K	G	-	-	31.9	9.9
1	K	L	K	L	K	M	V	V	S	W	T ₁	T ₂	15.7	7.7
2	K	L	K	L	K	M	V	V	S	W	T ₁	T ₁	15.5	7.7
3	K	L	K	L	K	M	V	V	S	A	T ₁	T ₁	57.1	22.5
4	K	L	K	L	K	M	V	V	A	W	T ₁	T ₁	4.1	1.9
5	K	L	K	L	K	M	V	A	S	W	T ₁	T ₁	19.0	6.9
6	K	L	K	L	K	M	A	V	S	W	T ₁	T ₁	6.2	2.7
7	K	L	K	L	K	A	V	V	S	W	T ₁	T ₁	31.1	7.6
8	K	L	K	L	K	N*	V	V	S	W	T ₁	T ₁	2.6	1.3
9	K	L	K	L	K	N*	V	V	Y	W	T ₁	T ₁	2.9	1.3
10	K	L	K	L	K	N*	V	V	A	W	T ₃	T ₁	1.2	0.2
11	K	L	K	L	K	N*	V	L	A	W	T ₃	T ₁	10.6	0.6
12	K	L	K	L	K	N*	V	I	A	W	T ₃	T ₁	9.1	0.9
13	K	L	K	L	K	N*	V	F	A	W	T ₃	T ₁	8.6	0.7
14	Q	L	K	L	K	N*	V	V	A	W	T ₃	T ₁	38.4	2.6
15	K	Q	K	L	K	N*	V	V	A	W	T ₃	T ₁	24.8	3.0
16	K	L	Q	L	K	N*	V	V	A	W	T ₃	T ₁	13.3	2.4
17	K	L	K	Q	K	N*	V	V	A	W	T ₃	T ₁	17.4	1.6
18	K	L	K	L	Q	N*	V	V	A	W	T ₃	T ₁	18.9	5.3
19	K	L	K	L	K	N*	A	V	A	W	T ₃	T ₁	11.5	0.5
20	K	L	K	L	K	N*	V	V	A	W	T ₁	T ₃	14.3	1.1
21	K	L	K	L	K	N*	V	V	A	W	T ₃	T ₃	26.9	10.3

Note: T₁ = NH₂CH₂CH₂N(SO₂Me)CH₂COOH; T₂ = L-Pro-D-Pro (Figure 1); T₃ = N(CH₂)₃CHCH₂OCH₂COOH; N* = Nle; Structure activity relationship of cyclic HYD1 derivatives in H929 myeloma cells. H929 cells were treated with varying concentrations of the indicated peptide for 24 hours. Cell viability was determined using Topro-3 staining and FACS analysis after drug treatment. IC₅₀ values were generated from linear regressions generated from the dose response curves (n = mean of at least 3 independent experiments). HYD1 (kikmviswkg) is a linear peptide, made of D-amino acids.

(ECM) proteins or to human dermal fibroblasts.^[11] The cyclic peptide **9** (N*VVYW) was synthesized with a design similar to the one found in the RZ-3 core sequence of the recognition strand, but the activity did not improve relative to peptide **8**.

Cyclic HYD1 peptide design was further improved by bringing additional restraint into the cyclic peptide by introduction of a constrained turn promoter T₃ (Figure 1) at one turn and the more flexible methylsulfonamide aminoethyl glycine linker T₁ (Figure 1) as the other turn. The introduction of an ether-peptidomimetic amino acid (*D*-prolinol derivative) as a constrained turn promoter was supported by conformational search and energy minimization studies that suggested the introduction of just one five membered ring *D*-Pro derived ether-peptidomimetic along with the somewhat more flexible turn geometry around the ether linkage as compared with *D*-Pro-*L*-Pro was favorable in stabilizing and sustaining the intramolecular hydrogen-bonding within the cyclic HYD1 analog. Based on this information, we synthesized the cyclic HYD1 peptide analog **10**, which had an IC₅₀ of 1 μ M. This peptide provided our best lead scaffold, MTI-101.

The antiparallel amphipathic strand of the cyclic HYD1 peptide was also varied. A side chain anchoring strategy was explored for easy preparation of this series of cyclic peptides. Various research groups

have applied this solid phase strategy to synthesize cyclic peptides.^[22-24] This strategy involves side chain anchoring of trifunctional amino acids such as Lys, Glu, Gln, Asp, or Asn for peptide elongation and on resin peptide cyclization. A sequential Gln substitution analysis on the amphipathic strand of the cyclic HYD1 analogs (peptides **14-18**) revealed that these residues significantly decreased the IC₅₀ of the peptide. The similar bioactivity observed for the cyclic *D*-HYD1 and the cyclic HYD1 peptide **1** suggests extensive peptide backbone interactions are absent or minimal since these two analogs have opposite backbone sequences. Efforts have been made to further enhance the bioactivity by varying hydrophobicity in the recognition strand of the lead peptide by incorporating hydrophobic residues at position 9 (peptides **11-13**). Efforts have been made to further enhance the bioactivity of lead peptide **10** by incorporating T₃ linkers at both turns (peptide **21**), but that was not promising.

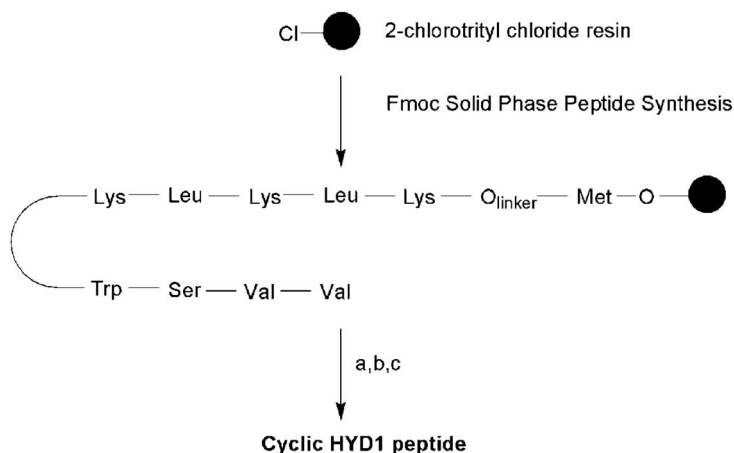
3.3 | Synthesis of linkers and cyclic HYD1 peptides

Cyclic peptides **1-9** were synthesized on 2-chlorotrityl chloride resin as solid support and Fmoc solid phase peptide synthesis strategy was

used as shown in Scheme 1. The linear peptides were synthesized and selectively cleaved from the resin without cleaving the side chain Boc-groups using trifluoroethanol as the cleaving agent. The linear peptide was then cyclized in solution under dilute conditions to afford crude cyclized peptide in modest yields. In order to synthesize a series of cyclic HYD1 peptide analogs with better yields, a peptide cyclization on resin approach using a side-chain attachment strategy was used for preparing peptides **10-13** and **19-21**. As shown in Scheme 2, the N^ε-amino group of the Lys was attached to 4-nitrophenyl carbonate derivatized Wang resin. The α-carboxyl group was protected with an orthogonal allyl ester protecting group. After synthesis of the protected linear peptide using standard Fmoc-based strategy, the C-terminus α-carboxyl group and the Fmoc group from the N-terminus were deprotected. The linear peptide was then cyclized on resin and subsequently released from the resin using TFA. For the

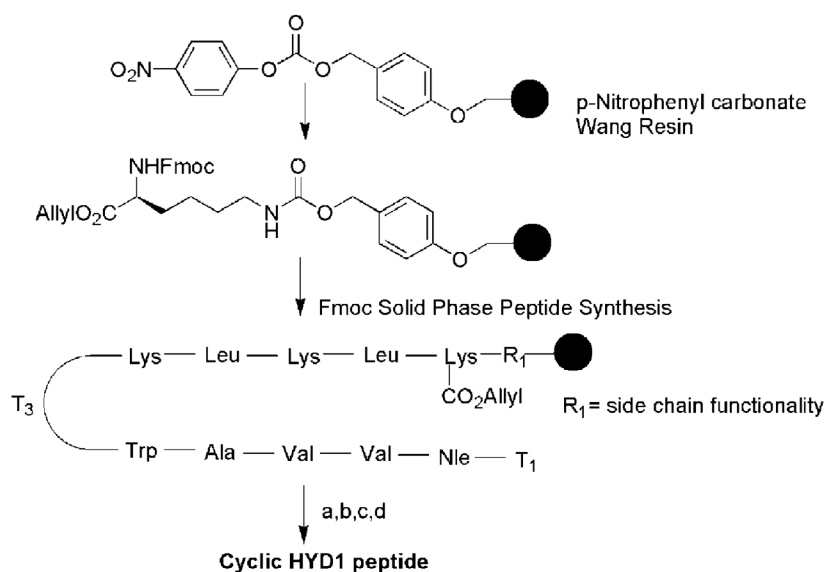
Gln scan of peptides **14-18**, we anchored the γ-side chain carboxyl group of Glu to Rink amide resin. The on-resin cyclization strategy of synthesizing cyclic peptides enabled us to synthesize and screen a moderate library of cyclic peptides very efficiently and in excellent yields (see Table S1).

Scheme 3 describes the synthesis of the methylsulfonamide aminoethyl glycine linker T₁. Selective mono-alkylation of excess ethylene diamine with tert-butyl bromoacetate was carried out under dilute conditions to give compound **2** in 85% yield.^[25] Compound **2** was used in the next step without further purification and selective Fmoc protection of the primary amine was achieved to give crude Fmoc-protected aminoethyl glycinate **3**. The crude reaction was washed with dilute hydrochloric acid and stored overnight at -20 °C, which resulted in the precipitation of pure compound **3** as the hydrochloride salt that can be stored for several months at 5 °C without



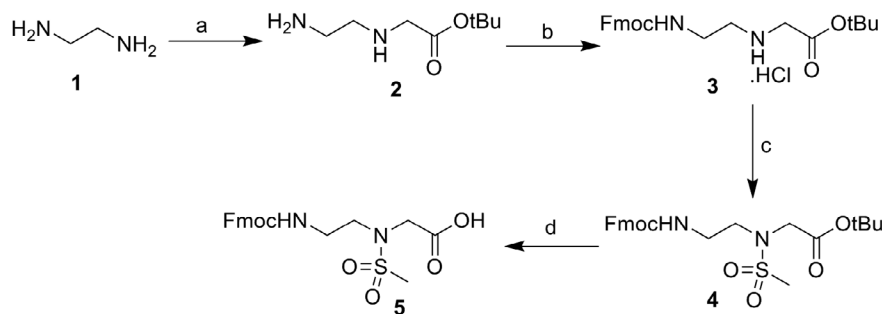
SCHEME 1 Solid-phase synthesis of cyclic HYD1 peptide using solution phase cyclization strategy

(a) 20% Trifluoroethanol in DCM, rt (b) HATU, DIEA, DMF (c) 95% TFA, Et₃SiH, H₂O



SCHEME 2 Solid-phase syntheses of cyclic HYD1 peptide analogs using a side chain anchoring strategy

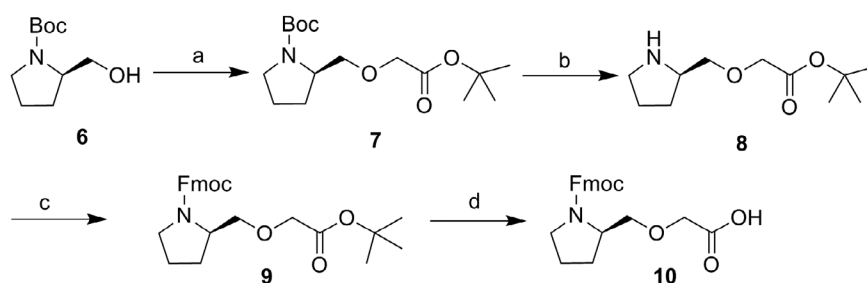
(a) 20% Piperidine/2% DBU in DMF, rt (b) Pd(PPh₃)₄ in CHCl₃-AcOH-NMM (37:2:1) (c) HCTU, DIEA, DMF (d) 95% TFA, Et₃SiH, H₂O



SCHEME 3 Synthesis of the methylsulfonamide aminoethyl glycine linker T_1

(a) $\text{BrCH}_2\text{CO}_2\text{tBu}$, THF, 85% (b) FmocNOSu, DIEA, DCM, 90% (c) MeSO_2Cl , DIEA, THF, 88%

(d) 1,4-Dioxane, 4M HCl, quant.



SCHEME 4 Synthesis of the ether peptidomimetic amino acid linker T_3

(a) NaOH, toluene, $\text{BrCH}_2\text{CO}_2\text{t-bu}$, TBAI, 77% (b) TFA/DCM (4:1) quant. (c) FmocOSu, DIEA,

DCM, 79% (d) TFA/DCM, Triethylsilane, quant.

decomposing. Mesylation of the secondary amine with methanesulfonyl chloride afforded compound **4** in good yields. Deprotection of the *t*-butyl group was achieved using 4 M $\text{HCl}_{(\text{g})}$ in 1,4-dioxane to give the desired compound **5** in excellent yields. The ether peptidomimetic amino acid linker T_3 was prepared from commercially available Boc-*D*-prolinol (Scheme 4). O-alkylation of **6** with tert-butyl bromoacetate afforded compound **7** in 77% yield. Selective removal of the Boc protecting group in compound **7** using trifluoroacetic acid in DCM (1:4) gave compound **8**. Fmoc protection of the secondary amine with Fmoc-OSu followed by acidic cleavage of the tert-butyl ester group gave the *D*-Pro derived ether-peptidomimetic **10** in 79% yield.

3.4 | Structural determination of cyclic peptides

3.4.1 | NMR studies for structural determination of cyclic peptides in solution

Complete peak assignments were only done for cyclic peptides **1**, **5**, and **10**. Assignments for both the recognition sequence and the non-recognition sequence, omitting the turns, were done for the remainder of the peptides. In an effort to reduce spectral overlap of the 2D

spectra sets, the NMR experiments were run in 100% D_2O to remove the exchangeable amide and Lys ϵ -NH protons from the spectrum. Even without information from the amide and Lys ϵ -NH protons, the results from our NMR experiments are consistent with the peptides having adopted a β -hairpin-like structure.

Our NMR results agree with previous empirical analysis which has shown that when extended conformations are formed, there is a downfield shift in the H_α resonances.^[26,27] The majority of the amino acid H_α 's in our peptides are shifted significantly downfield such that their values indicate a β -hairpin conformation (Table 2).

H_α and NOE NMR analysis of peptide **1**, which contains both the Robinson β -hairpin turn promoter template (*D*-Pro-*L*-Pro) and the methylsulfonamido aminoethyl glycine turn, suggests the structure of this peptide as a β -sheet.^[20] This peptide was cyclized using a methylsulfonamido aminoethyl glycine in place of the *D*-Pro-*L*-Pro as the β -hairpin turn promoter to give peptide **2**. A comparison between the H_α shifts of these two peptides reveals many similarities. Most of the H_α 's on the amphipathic strand of peptide **2** have shifted upfield relative to **1**, suggesting that the structure is less like a β -sheet. While three of these residues have only shifted about 0.2 ppm or less upfield, Leu4's shift of about 0.7 ppm suggests a fair amount of structural change. The only H_α on the amphipathic strand that has a downfield shift is Lys5. More importantly however, all but one of the H_α 's

TABLE 2 α -proton chemical shifts (ppm) of selective cyclic peptide analogs

	Position											
	R ₁	R ₂	R ₃	R ₄	R ₅	R ₆	R ₇	R ₈	R ₉	R ₁₀	R ₁₁	R ₁₂
1	4.38	4.54	4.29	4.99	4.54	4.48	4.13	4.27	4.60	4.69	3.56 ^S 3.86 ^R	L-Pro 4.53 D-Pro 4.74
2	4.26	4.35	4.08	4.28	4.57	4.64	4.66	4.32	4.46	4.70	—	—
5	4.31	4.16	4.07	4.04	4.42	4.60	4.58	4.53	4.60	4.61	3.89 ^S 4.06 ^R	3.47 ^S 4.05 ^R
7	4.44	4.31	4.08	4.28	4.52	4.42	4.63	4.18	4.70	4.67	—	—
8	4.29	4.29	4.09	4.38	4.59	4.45	4.67	4.64	4.45	4.60	—	—
10	4.55	4.78	4.32	4.63	4.17	4.34	4.44	4.55	4.70	5.05	4.23	3.94 ^S 4.08 ^R

Abbreviations: R, Pro-R; S, Pro-S.

on the hydrophobic strand of the peptide have shifted downfield indicating a β -sheet conformation. The H $_{\alpha}$ of Ser9 is the only one that has shifted upfield. Looking at the fact that the H $_{\alpha}$'s on residues Met6 and Lys5 have shifted downfield after the β -hairpin turn promoter was changed from the *D*-Pro-*L*-Pro to our methylsulfonamido aminoethyl glycine turn, it suggests that the methanesulfonamide turn promoter allows for more β -hairpin-like character at this end of the peptide. Thus, this turn promoter may be a better β -hairpin promoter for certain peptide sequences.

Although most of the H $_{\alpha}$ shifts were small, about 0.2 ppm or less, there was a large shift in two of the H $_{\alpha}$'s which appears to be structurally significant. While the Leu4's H $_{\alpha}$ shifted upfield 0.70 ppm, Val7's H $_{\alpha}$ shifted downfield 0.53 ppm. This suggests that the Leu4 is not adopting a predominantly β -sheet conformation. This is most likely due to steric interactions from the γ -protons of Val7 which is directly across from Leu4. Presumably as a direct result of Leu4's structural conformational change, Lys3's H $_{\alpha}$ is shifted 0.22 ppm (the second largest shift) upfield.

An examination of the other peptides reveals a similar phenomenon. The Leu4 H $_{\alpha}$ is shifted upfield and the residue in position 7 is shifted downfield in comparison with peptide **1**. This can be explained by the fact that the *D*-Pro-*L*-Pro turn in the Robinson template is structurally rigid, forcing those residues proximate to it. The methylsulfonamido aminoethyl glycine turn is probably more flexible, thus allowing the residues close to the turn to be less rigid. It is probably this flexibility that allows the Leu4 H $_{\alpha}$ to deviate from the β -sheet configuration. NOE analysis supports this view. In peptide **1**, strong NOEs were observed between the H $_{\alpha}$'s of Leu4 and Val7. However, in peptide **2** the NOE between the H $_{\alpha}$'s of Leu4 and Val7 was only of low intensity. In its place, there was a semi-strong NOE between the H $_{\alpha}$ of Leu4 and one γ -CH₃ groups of Val7. This significant reduction in the NOE cross-peak intensity between the Leu and Val H $_{\alpha}$'s combined with the appearance of a new strong cross-peak between the Leu H $_{\alpha}$'s is strong evidence in support of the flexibility of our turn relative to the *D*-Pro-*L*-Pro turn (see Tables S2, S3, and Figure S1).

We also investigated the other ether peptidomimetic amino acid linker (T₃) as a β -turn promoter. This promoter is similar to the *D*-Pro-

L-Pro turn in that they both contain pyrrolidine rings however; T₃ has a higher degree of flexibility than the *D*-Pro-*L*-Pro turn due to T₃ containing only one ring and it lacks the additional carbonyl group. An empirical analysis of the H $_{\alpha}$'s in peptide **10** shows more resonances adopting a β -sheet conformation than any other peptide. This suggests that the T₃ linker is capable of promoting a β -turn while retaining some flexibility that allows more residues to adopt a β -sheet.

Comparing the H $_{\alpha}$'s of peptides **1** and **10** reveals a number of striking similarities and further demonstrates linker T₃'s ability to induce a β -turn. Focusing on the amphipathic strands, a comparison of the H $_{\alpha}$ of the Lys residues closest to their respective turns (**1** Lys5 vs **10** Lys1) reveals almost no chemical shift difference outside of experimental error. Moving further away from the respective turns, the chemical shift difference between the two Lys3 H $_{\alpha}$'s increases slightly to 0.029 ppm implying **10** has slightly more β -sheet character at this residue. Generally, as is the case for **1**, the H $_{\alpha}$ of the Lys furthest from the turn is slightly downfield of Lys3's H $_{\alpha}$. In peptide **10**, however, Lys5's H $_{\alpha}$ is considerably upfield of Lys3. Additionally, the H $_{\alpha}$'s of both Lys5 and Nle6 in **10** are significantly upfield of the same protons in peptide **8** (see Tables S6 and S7). Combined, these facts show that this end of the turn, from Lys5 through the turn to Nle6, adopts slightly less of a β -sheet conformation in **10**. This is most likely caused by relieved conformational strain generated by the methylsulfonamido aminoethyl glycine turn. It should be noted however that all of the protons in the T₁ linker of **10** have been significantly shifted downfield relative to those in the T₁ linker of **1**, suggesting the superiority of the T₃ linker over the Robinson turn.

Moving on to the hydrophobic strand, there is a downfield shift of Trp's H $_{\alpha}$ in **10** vs **1** which is probably due to its proximity to the β -turn. With regards to the Val residues, we would expect them to follow a similar trend. The H $_{\alpha}$'s for both Val7 and Val8 in **10** are shifted significantly downfield (0.28 and 0.31 ppm, respectively) from those in peptide **1**. In a comparison of the H $_{\alpha}$'s of the Val8 residues between the two peptides, we would expect their H $_{\alpha}$ chemical shifts to be fairly similar given their central location on the hydrophobic strand of the peptide. This however is clearly not the case, which indicates that **10**'s hydrophobic strand contains more β -sheet character at this residue

than in peptide **1**. Therefore, extrapolation of these findings indicates that the entire hydrophobic strand in peptide **10** has adopted a β -sheet conformation.

The replacement of the Robinson template by the turn T_1 slightly increases the distance between the two sides of the β -sheet. This change in distance can be seen by the decrease in NOE intensity between the Leu and Val residues mentioned previously. NOEs also show the disappearance of the following: a strong NOE between the ϵ protons of Met6 and the H_α of Lys5, a strong NOE between the γ_1 protons of Val8 and the β and β' protons of Lys3. Also, the intensity of the NOE interaction between the γ_2 protons of Val8 and the β proton of Lys3 dropped from being semi-strong to being weak upon replacement of the Robinson turn.

3.4.2 | Peptide structural characterization via NOE

In conjunction with the chemical shifts of the α -protons, the NOE data was used to help determine the 3D structure of peptides. Figures 2 and 3 show the NOEs found for peptides **2** and **5** respectively. Analysis of peptide **5** was used as a general model for all the peptides. Cross-strand analysis reveals many NOEs between the Trp10 and Lys1 residues, specifically between Trp4H-LyseH, Trp5H-Lys β H, Trp5H-LyseH, Trp6H-Lys γ H, and Trp β H-LyseH to name a few. These suggest that the Tryptophan ring sits between the two strands at an angle with the indole ring facing the rest of the peptide. Additionally, peptide **2** also shows a NOE between Trp β H-Lys β H, evidence that the ring spends part of its time in an alternate position between the two strands.

Chemical shift analysis supports these two Trp positions, showing that the Tryptophan ring occupies one of the two positions depending on the adjacent residues. With the exception of the H_α 's, all of the

protons in Lys1 are downfield of their respective ones in either Lys3 or Lys5 even though Lys1 is cross-strand from Trp10 which would suggest an upfield shift due to an interaction with the face of the aromatic rings. The first, and main, position Trp occupies is one that deals with those peptides that contain a Valine at residue 8. Here, the aromatic ring of Trp10 and the hydrophobic γ -methyl groups of Val8 are oriented with each other such that one face of the Tryptophan ring is interacting with the Valine via intra-pair van der Waal's contacts while the other face is interacting with the Lys1 protons via cation- π interaction causing the γ -methyl's to slightly shift upfield. This is consistent with the chemical shifts of the Valine in position 8 because the protons interacting with the Tryptophan ring shift upfield relative to their proximity to the Tryptophan ring as is expected due to the increased shielding from the ring. However, peptide **7** does not follow this model. While the Val8 H_α does shift upfield, the β and γ -protons shift downfield which means the face of the Tryptophan ring is not interacting with that Valine to the same extent as the other peptides (see Table S5). This downfield shift is also seen in peptide **10**. In peptide **7**, all of Lys3's protons shift upfield with the exception of the H_α and new prominent NOEs can be seen between Lys3 and Trp10 (see Figure S2). This combined with the fact that there was very little shift, up or downfield, of Lys1's protons means the faces of the Tryptophan ring are now interacting with Lys 1 and Lys3 rather than with Lys1 and Val8. This is probably due to the replacement of the Methionine with an Alanine at position 6 thus reducing the van der Waal's interactions and reducing the hydrogen bonding between positions 3 and 6.

The second position Trp occupies is found in peptide **5**, which lacks a Valine at residue 8. Here, the Tryptophan ring sits between the two strands partially over the turn and is at an angle with the indole ring facing the rest of the peptide. In this orientation, there is less interaction between the face of the Tryptophan ring and the protons

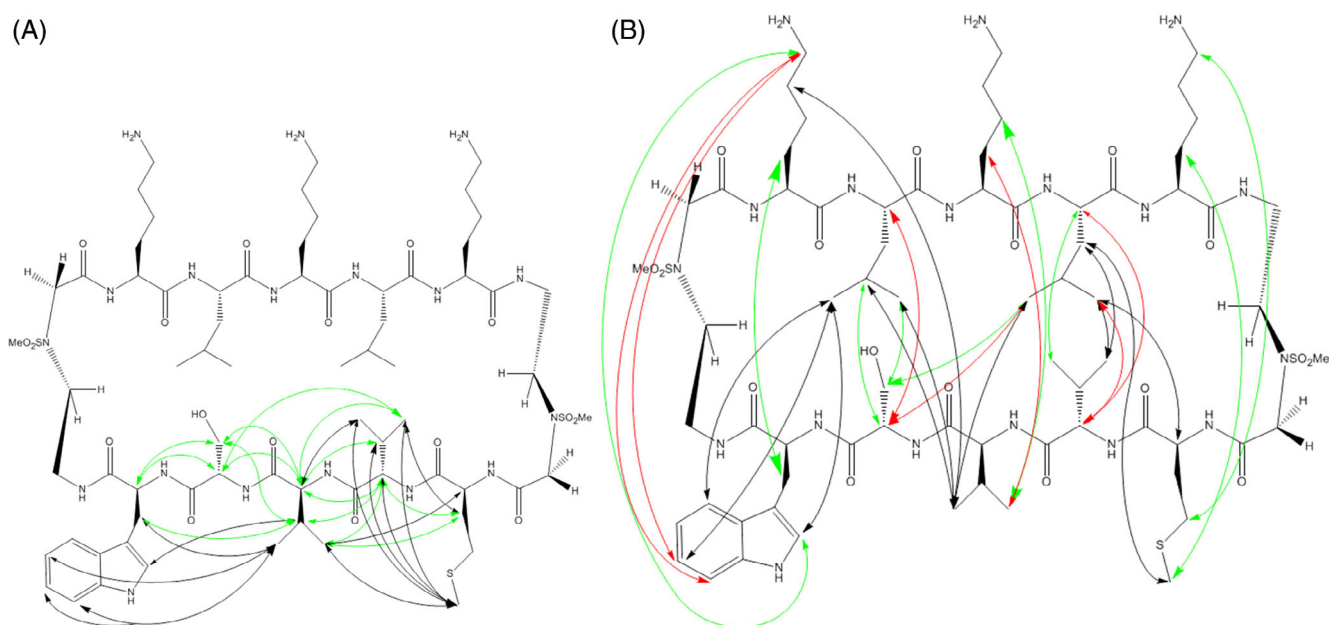


FIGURE 2 Peptide **2** NOEs: A, Same-strand NOEs; B, Cross-strand NOEs (black, strong; green, medium; red, weak)

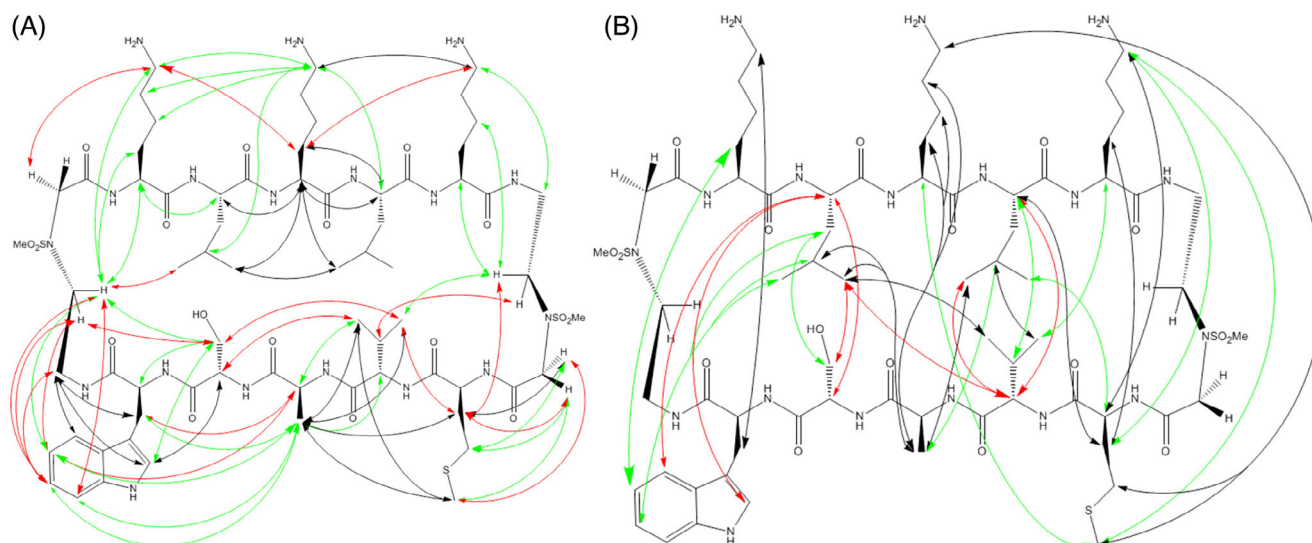


FIGURE 3 Peptide 5. NOEs: A, Same-strand NOEs; B, Cross-strand NOEs (black, strong; green, medium; red, weak)

of Lys1. Therefore, the Lys1 resonances are shifted slightly downfield. Regardless of the presence or absence of a Valine at residue 8, the Lys5 and Lys3 resonances are more upfield due to interactions with each other and the Methionine (see Table S4).

Interestingly, peptide 5 shows only a small NOE between the H_α's of Leu2 and Ser9, much like the Leu4-Val7 interaction mentioned above. There are however a few notable NOEs between Leu2 and Ser9 which include SerβH-LeuδH, SerβH-LeuβH, and SerβH-Leuβ'H. These imply that the Leucine is oriented such that the β-protons point into the β-sheet while the δ-methyl protons are pointing down and away from the β-sheet. It is also important to note the chemical shift of the Serine H_α. There is no difference in the Serine H_α chemical shift between peptides 1 and 5. This is due to the fact that in 1, the Robinson turn helps to keep everything in a tight β-sheet and so the Serine H_α is most likely artificially changed due to the Tryptophan ring current effects while in 5, the Tryptophan ring is over the turn. However, in peptides 2 and 8, the Tryptophan ring is above the Serine H_α shielding it and causing an upfield shift. In peptide 7, the Serine H_α is significantly downfield suggesting that the Tryptophan ring is not sitting above it; this is supported by the NOE data. NOE data for peptide 10 suggests that while the Tryptophan ring is over the β-sheet, it may be in a more vertical position over Leu2 and Ala9 interacting with the Lys1 and Lys3 side chains (see Figure S4). This possible ring orientation is supported by the downfield shift of Alanine's H_α.

In peptide 5, the NOEs between the Ala8 and Lys3 residues are of significant intensity. The Alanine β-proton shows an NOE with the β, β', γ, and δ-protons of Lys3. Although the other peptides possess a Valine at position 8, they show the same NOEs with Lys3 and some even show NOEs to Lys1 and Lys5. These cross-strand and diagonal cross-strand NOEs imply that all of the Lysine's are oriented over the β-sheet itself and that when there is a Valine in position 8, its γ-methyl groups are aligned with the β-sheet and point in opposite directions.

The Valine in position 7 has several cross-strand NOEs, while most are with Leu4 there is one with Leu2 which is quite intense. A few of those with Leu4 include Val₂H-Leu₇H, Val₂H-Leu₇δH, Val₂H-Leu₇βH, ValβH-Leu₄αH, and ValαH-Leu₇δH. The NOE with Leu2 is between Val₇H and Leu₂δH. Although the intensity of the NOE between the H_α's of Val7 and Leu4 is quite low, the strengths of the NOEs just mentioned provide compelling evidence that the structure of this part of the peptide is indeed a β-sheet.

NOEs from peptide 5's Met6 describe an interesting side-chain shape and a particular orientation with Lys5. Some of these include MetεH-LysαH, Metβ'H-Lysβ'H, Metβ'H-LysεH, and MetαH-LysεH. Since these residues are attached to either side of the turn, their cross-strand NOEs are proof that the turn does in fact make a β-sheet rather than a random coil. Additionally, NOEs are also observed between Met6 and Lys3. Some of the most significant ones are MetεH-LysεH, MetγH-LysεH and MetβH-LysεH. These diagonal cross-strand NOEs help to reinforce the fact that these peptides exist as β-sheets despite the lack of a strong NOE between the H_α's of Leu4 and Val7. These NOEs suggest that the Methionine side chain is specifically interacting with these two Lysine side chains. In addition to the standard Van der Waals interactions, weak hydrogen bonding may exist between the Methionine sulfur and the Lysine ε-NH protons holding the chains closer in space thus giving rise to more and stronger NOEs between the chains. This idea is supported by the fact that when Methionine is replaced by Norleucine in 8, both the amount and the intensity of the cross-strand NOEs decrease significantly. Furthermore, both the ε and γ-methylenes of Lys5 experience a significant downfield shift upon the replacement with Norleucine. Replacing the Methionine residue with a more hydrophobic one removes the hydrogen bonding and causes a change in the side chain conformation, which is evident in peptide 8 (see Figure S3).

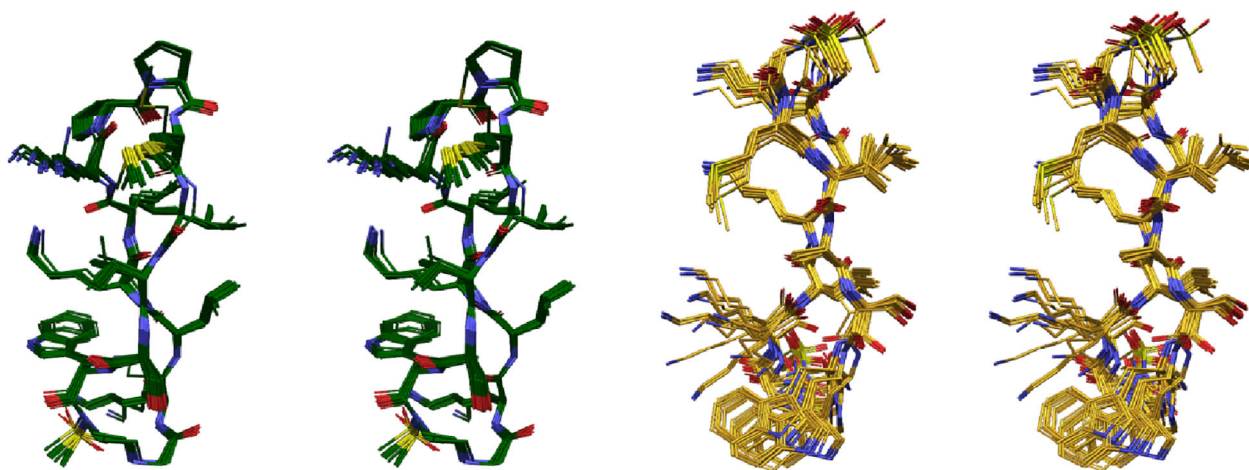


FIGURE 4 Stereoviews of the 20 lowest energy structures for NOE-constrained calculated structure of peptides **1** (green carbon atoms) and **5** (gold carbon atoms). N, blue; O, red; S, yellow; hydrogens omitted for clarity. Thin wire representations prepared with Maestro

3.4.3 | Constrained conformation search with MacroModel

Structures of peptides **1** and **5** were built with Maestro.^[17] NOE-derived distance constraints were applied to optimize the peptide structures with MacroModel to produce 891 and 920 structures within a 100 kJ/mol range for peptides **1** and **5**, respectively.^[18] The conformations were reduced in number based on RMSD to 61 and 87 structures of which the 20 lowest energy representative structures shown in Figure 4 were analyzed. Both sets of calculated structures reveal a twisting of the β -hairpin structure. Further, peptide **1** has a more subtle twist close to its rigid *D*-Pro-*L*-Pro linker while the β -hairpin is more contorted near linker T_1 . The Ramachandran plot places all phi/psi angles of peptide **5** in the β -sheet region while 2 amino acids, *L*-Pro and Val 7, of peptide **1** are in the disallowed region (see Figure S5). The averaged energies offer explanation to these structural differences: solvation and electrostatics contribute 80% of the difference in the average energies of the calculated structures (see Table S9). The flexibility of the linker T_1 in comparison to the rigid *D*-Pro-*L*-Pro linker allow for a more solvated conformation when in solution, an entropic gain (from less ordered waters) that translates into lower electrostatic and solvation energies. Further, peptide **5** has lower stretch, bend, and torsion energies than peptide **1** accounting for less than 20% of the average energy difference (see Table S9). Overall, the average energies from the calculated structures indicate more conformational flexibility of peptide **5** over peptide **1** (see Table S8).

3.4.4 | Conformational studies of cyclic peptides using CD

CD is a sensitive measure of the secondary structure of peptides and proteins. CD spectroscopy measures the difference in absorbance of

right- and left-circularly polarized light by a substance. Peptides usually show absorption in the ultraviolet region of the spectrum from the peptide bonds and side chains of the amino acids in the sequence. Various reports cited in the literature have shown that CD spectra from 260 to 190 nm were analyzed for the different structural of peptides and proteins that is, α -helix, parallel and antiparallel β -sheet, β -turn, etc.^[28,29] The lowest energy transition in the peptide chromophore is an $n \rightarrow \pi^*$ transition observed at 210 to 220 nm with weak intensity. The peptide with beta-sheet structure usually exhibits an absorption minima around 210 nm and a relatively strong absorption maxima around 190 nm. Peptide conformational studies using CD are mainly characterized by comparing analysis of overall shape of the CD spectra with standard peptide spectra. The conformational study of cyclic peptides was carried out in buffered aqueous solutions (see Figure S6). These cyclic peptides displayed similar, but different characteristic CD bands: negative absorption minima around 200 nm and strong positive absorption maxima around 185 to 190 nm. These characteristic CD bands are indicative of a β -sheet or β -turn secondary structures. These peptides show strong absorption at higher concentration indicating a possible dimeric or oligomeric species in aqueous buffered solutions.

4 | CONCLUSIONS

Cyclic HYD1 peptides containing core residues of parent linear HYD1 in the hydrophobic strand and an amphipathic strand were synthesized using a novel methylsulfonamide aminoethyl glycine linker T_1 and an ether peptidomimetic amino acid linker T_3 as turn promoters. Robinson's *D*-Pro-*L*-Pro turn in peptide **1** is very structurally rigid, whereas the methylsulfonamide aminoethyl glycine linker T_1 is more flexible. NMR (α -proton chemical shifts and NOE analysis) studies show clear evidence of these cyclic peptides adopting a β -hairpin-like conformation. Cyclic HYD1 peptides with one T_3 and one T_1 linker

provide a lead scaffold having high potency against MM *in vitro*. On-resin cyclization of linear peptide fragments is efficient, and the resulting cyclic peptides are easily purified. SAR studies on the cyclic HYD1 peptide indicate that Trp, Val, and Nle are critical residues responsible for increased potency of the peptide. The amphipathic strand also appears critical. Cyclic HYD1 peptide **10** or MTI-101 shows promising *in vivo* activity described herein and its *in vivo* activity is reported independently.^[15,16]

ACKNOWLEDGMENTS

The authors thank the Multiple Myeloma Research Foundation and NIH (5R01CA195727 and 5R44CA22155) for grant support. We thank USF Peptide & Mass Spectrometry Facility for cyclic peptide synthesis.

CONFLICT OF INTEREST

S. Kaulagari is employed as a Senior Scientist in Modulation Therapeutics Inc. M. L. McLaughlin is co-founder/Executive Vice President and has ownership interest (including patents) in Modulation Therapeutics Inc. L. A. Hazlehurst is co-founder/president and has ownership interests (including patents) in Modulation Therapeutics Inc. No potential conflicts of interest were disclosed by the other authors.

AUTHOR CONTRIBUTIONS

Lori A. Hazlehurst, Mark L. McLaughlin: Conception and design. **Priyesh Jain, Yi Liang, Sridhar R. Kaulagari, Philip Murray, MohanRaja Kumar, Ted J. Gauthier:** Synthesis of peptides. **David Badger:** NMR analysis of peptides. **Anthony W. Gebhard, Rajesh Nair, Priyesh Jain:** Acquisition of data (provided animals, acquired and managed facilities, etc.). **Daniel Santiago, Wayne C. Guida:** Computational analysis. **Priyesh Jain, Sridhar R. Kaulagari, Mark L. McLaughlin, Lori A. Hazlehurst:** Writing, review and/or revision of the manuscript. **Anthony W. Gebhard, Lori A. Hazlehurst, Mark L. McLaughlin:** Study supervision.

DATA AVAILABILITY STATEMENT

The data that supports the findings of this study are available in the supplementary material of this article.

ORCID

Mark L. McLaughlin  <https://orcid.org/0000-0002-7329-2038>

REFERENCES

- [1] R. E. Durand, R. M. Sutherland, *Exp. Cell. Res.* **1972**, *71*, 75.
- [2] J. S. Damiano, A. E. Cress, L. A. Hazlehurst, A. A. Shtil, W. S. Dalton, *Blood* **1999**, *93*, 1658.
- [3] J. S. Damiano, W. S. Dalton, *Leukemia & Lymphoma* **2000**, *38*, 71.
- [4] J. S. Damiano, *Curr. Cancer Drug Targets* **2002**, *2*, 37.
- [5] L. A. Hazlehurst, W. S. Dalton, *Cancer Metast. Rev.* **2001**, *20*, 43.
- [6] L. A. Hazlehurst, T. H. Landowski, W. S. Dalton, *Oncogene* **2003**, *22*, 7396.
- [7] M. B. Meads, L. A. Hazlehurst, W. S. Dalton, *Clin. Cancer Res.* **2008**, *14*, 2519.
- [8] M. F. Emmons, A. W. Gebhard, R. R. Nair, R. Baz, M. L. McLaughlin, A. E. Cress, L. A. Hazlehurst, *Mol. Cancer Ther.* **2011**, *10*, 2257.
- [9] W. L. Harryman, N. A. Warfel, R. B. Nagle, A. E. Cress, *Adv. Exp. Med. Biol.* **2019**, *1210*, 149.
- [10] M. E. Pennington, K. S. Lam, A. E. Cress, *Mol. Diversity* **1996**, *2*, 19.
- [11] I. B. DeRoock, M. E. Pennington, T. C. Sroka, K. S. Lam, G. T. Bowden, E. L. Bair, A. E. Cress, *Cancer Res.* **2001**, *61*, 3308.
- [12] T. C. Sroka, J. Marik, M. E. Pennington, K. S. Lam, A. E. Cress, *Cancer Biol. Ther.* **2006**, *5*, 1556.
- [13] T. C. Sroka, M. E. Pennington, A. E. Cress, *Carcinogenesis* **2006**, *27*, 1748.
- [14] R. R. Nair, M. F. Emmons, A. E. Cress, R. F. Argilagos, K. Lam, W. T. Kerr, H. G. Wang, W. S. Dalton, L. A. Hazlehurst, *Mol. Cancer Ther.* **2009**, *8*, 2441.
- [15] A. W. Gebhard, P. Jain, R. R. Nair, M. F. Emmons, R. F. Argilagos, J. M. Koomen, M. L. McLaughlin, L. A. Hazlehurst, *Mol. Cancer Ther.* **2013**, *12*, 2446.
- [16] M. F. Emmons, N. Anreddy, J. Cuevas, K. Steinberger, S. Yang, M. McLaughlin, A. Silva, L. A. Hazlehurst, *Sci. Rep.* **2017**, *7*, 2685.
- [17] *Maestro*, Schrödinger LLC, New York, NY **2008** 8.5 ed.
- [18] *Macromodel*, Schrödinger LLC, New York, NY **2010** 9.8 ed.
- [19] T. A. Halgren, R. B. Murphy, R. A. Friesner, H. S. Beard, L. L. Frye, W. T. Pollard, J. L. Banks, *J. Med. Chem.* **2004**, *47*, 1750.
- [20] M. Favre, K. Moehle, L. Jiang, B. Pfeiffer, J. A. Robinson, *J. Am. Chem. Soc.* **1999**, *121*, 2679.
- [21] H. E. Stanger, F. A. Syud, J. F. Espinosa, I. Gariat, T. Muir, S. H. Gellman, *Proc. Natl. Acad. Sci. U. S. A.* **2001**, *98*, 12015.
- [22] M. Rabinowitz, P. Seneci, T. Rossi, M. Dal Cin, M. Deal, G. Terstappen, *Bioorg. Med. Chem. Lett.* **2000**, *10*, 1007.
- [23] C. M. Gross, D. Lelievre, C. K. Woodward, G. Barany, *J. Pept. Res.* **2005**, *65*, 395.
- [24] S. Ficht, R. J. Payne, R. T. Guy, C. H. Wong, *Chemistry* **2008**, *14*, 3620.
- [25] T. A. Feagin, N. I. Shah, J. M. Heemstra, *J. Nucleic Acids* **2012**, *2012*, 1.
- [26] D. S. Wishart, B. D. Sykes, F. M. Richards, *J. Mol. Biol.* **1991**, *222*, 311.
- [27] D. S. Wishart, B. D. Sykes, F. M. Richards, *Biochemistry* **1992**, *31*, 1647.
- [28] T. E. Creighton, *Protein: Structures and Molecular Properties*, 2nd ed., W. H. Freeman and Co., New York, NY **1993**.
- [29] L. Tilstra, W. L. Mattice, in *Circular Dichroism and the Conformational Analysis of Biomolecule* (Ed: G. D. Fasman), Plenum Press, New York, NY **1996**.

SUPPORTING INFORMATION

Additional supporting information may be found online in the Supporting Information section at the end of this article.

How to cite this article: Jain P, Badger DB, Liang Y, et al. Bioactivity improvement via display of the hydrophobic core of HYD1 in a cyclic β -hairpin-like scaffold, MTI-101. *Peptide Science*. 2021;113:e24199. <https://doi.org/10.1002/pep2.24199>